169 DOI: 10.5507/fot.2025.008

Mallomonas intermedia: A case study of speciation and evolutionary dynamics of protists

Pavel Škaloud^{1,*}, Magda Škaloudová¹, Petr Knotek¹, Iva Jadrná¹ & Martin Pusztai^{1,2}

Abstract: A total of 81 strains morphologically corresponding to the circumscription of Mallomonas intermedia were isolated from 27 freshwater localities across Europe and North America. Molecular genetic analyses revealed two distinct lineages with a strict geographical pattern, which diverged approximately 8 million years ago. According to comparative morphological analyses, we concluded that European populations corresponded to M. intermedia, whereas North American populations were described as a new species, M. retimedia sp. nov. The most notable morphological difference between the species is in the number of pores enclosed in the mesh formed on the siliceous scales. While in M. intermedia the mesh typically surrounds only one pore, meshes of M. retimedia usually encircle 3-4 pores. By incorporating fossil evidence into our time-calibrated phylogeny, we propose that the ancestor of M. intermedia and six related species likely lacked a thick secondary layer but had a distinct transverse rib, present in extant M. galeiformis, M. intermedia and M. retimedia species. The evolutionary history of this group further reveals that parallel ribs on the siliceous scales have evolved independently at least three times during the Miocene epoch, suggesting an adaptive significance, although their exact function remains unclear.

Key words: Chrysophyceae, evolution, microfossils, morphology, silica scales, speciation, Synurales

Introduction

Although eukaryotic microorganisms (protists) are incredibly numerous, diverse, and essential for global ecosystem functioning, they remain relatively understudied by evolutionary biologists compared to multicellular organisms (GERSTEIN & MOORE 2011). Due to their small sizes and the challenges associated with culturing them, our understanding of their evolutionary processes is significantly limited. In particular, the divergence processes that lead to the formation of evolutionary young protist species are poorly understood. A remarkable example of such rapid speciation is illustrated by the work of LOGARES et al. (2007) and Annenkova et al. (2015), who identified a group of morphologically distinct dinoflagellate species that emerged through recent, post-glacial adaptive radiation following the transition from marine to freshwater habitats. A similar, habitat-driven radiation has been observed in benthic diatoms in the ancient Lake Ohrid (STELBRINK et al. 2018), with several species emerging over the past 2 million years. In marine environment, the

haptophyte genus Gephyrocapsa Kamptner is among the most studied organisms regarding recent diversification events, with a well-preserved fossil record showing cyclical patterns of species radiations during the last 2 million years (BENDIF et al. 2019).

Numerous studies have identified patterns of recent genetic differentiation in both marine and freshwater freeliving protists, revealing geographical (Casteleyn et al. 2010; Rengefors et al. 2012; Tahvanainen et al. 2012), ecological (Postel et al. 2020; Škaloud et al. 2024), and temporal patterns (RYNEARSON et al. 2006; LEBRET et al. 2012). However, these genetically differentiated clusters are often morphologically indiscernible, making it challenging to determine whether they represent real young species entities. Indeed, the lack of distinct morphological features in many protist groups is a major obstacle in detecting recent speciation events. Nevertheless, some protists possess hard shells or skeletons with diverse structural formations that exhibit sufficient variability, providing valuable diagnostic characters to detect subtle morphological differences between recently diverging

¹Charles University, Faculty of Science, Department of Botany, CZ-12800 Praha, Czech Republic; *Corresponding author e-mail: skaloud@natur.cuni.cz

²Institute for Nanomaterials, Advanced Technologies and Innovation, Technical University of Liberec, Studentská 1402/2, CZ-46117 Liberec, Czech Republic

species (KNOLL & KOTRC 2015).

Silica-scaled chrysophytes (Stramenopiles, Chrysophyceae), an ecologically important group of freshwater phytoplankton algae, produce microscopic siliceous scales that cover their cells (SIVER 1991). The species concept for these organisms is traditionally based on the morphology of siliceous structures observed through electron microscopy, primarily focusing on various patterns found on siliceous scales, such as diverse reticulations, ribs, papillae, pores, and pits (Kristiansen 2005; SIVER 2015a). Recent diversification events have been primarily studied in the colonial genus Synura Ehrenberg, where a significant species flock has been uncovered within the section Petersenianae (ŠKALOUD et al. 2012, 2014). A total of 29 species or species-level lineages have been identified in this flock (JADRNÁ & ŠKALOUD 2025), radiating over the last 10 million years (ŠKALOUD et al. 2020). While some of these recently diverged species are morphologically distinguishable by features such as large pores or elongated scales, the majority are highly similar, differing only by fine morphological differences. Another adaptive radiation was uncovered within the species Synura sphagnicola (Korshikov) Korshikov, which radiated into several ecologically and geographically distinct lineages during the late Pleistocene (ŠKALOUD et al. 2019). However, due to the lack of morphological features distinguishing these lineages, they were described as sub-species (ŠKALOUD et al. 2023).

Interestingly, no study focusing on recent diversification has been performed so far on the most species—rich genus of silica scaled chrysophytes, the unicellular genus *Mallomonas* Perty. Despite numerous new species being described every year, only a portion of these studies includes molecular data to supplement the species descriptions. Time—calibrated analyses indicate that although some morphologically similar species appear to have undergone rapid diversification, they typically originated much earlier, around 20–50 million years ago (Jo et al. 2013).

Recently, an intriguing observation was published by SIVER et al. (2019), discovering a putatively European endemic species, Mallomonas intermedia Kisselev, in a small, shallow, man-made pond in Nevada, USA, as well as in a stratigraphic sequence from the middle Eocene fossil locality known as Horsefly in British Columbia, Canada. In their detailed study, SIVER et al. (2019) conclusively changed the status of M. intermedia to a palaeoendemic species, since this organism and its plausible close relatives (M. lancea Siver, Lott et Wolfe and M. dispar Siver, Lott et Wolfe) were present in North America during the Eocene, over 48 million years ago. Unfortunately, no molecular data were available to genetically compare extant European and American populations, leaving an intriguing question about their taxonomic status. While minor differences in the reticulation on the shield of scales have been presented by SIVER et al. (2019), it remains unclear whether these populations represent a single species with a broad distribution or two closely related, recently radiating species with more restricted ranges. This study aims to address this question through both genetic and morphological analyses of *M. intermedia* populations isolated from North America and Europe, ultimately revealing the taxonomic status of these organisms.

MATERIALS AND METHODS

The strains analysed in this study originated from the extensive Mallomonas sampling that took place between 2020 and 2025 in various European and North American sites. Plankton net samples were taken from various habitats using a plankton net with a 20 µm mesh. Samples were examined with an Olympus CH light microscope and individual cells were isolated by micropipetting into a separate well of a 96-well polypropylene plate filled with approximately 300 ml of liquid MES or TES buffered WC medium (GUILLARD & LORENZEN 1972) with the addition of soil extract. The plates were cultivated at 14 $^{\circ}$ C under constant illumination of 40 μ mol photons m $^{-2}$. s $^{-1}$ (TLD 18 W/33 fluorescent lamps; Philips). After 3-4 weeks the wells were checked using an inverted microscope Leica DMi1 and 100 µl of the culture was harvested for genotyping by ITS rDNA barcode. Selected strains were inoculated into 50 ml Erlenmeyer flasks filled with the same medium and grown as described above.

Live Mallomonas cells were observed and photographed using an Olympus BX51 light microscope equipped with Nomarski interference contrast and a Canon EOS 700D camera. For measurements of scales and bristles, small drops of both the cultures and fresh plankton samples were applied onto Formvar supported grids and air-dried, washed with distilled water and re-dried. The material was observed with a JEOL 1011 transmission electron microscope equipped with a CCD camera Veleta with acquisition software (Olympus Soft Imaging Solution GmbH, Münster, Germany). Almost 100 scales were measured to determine their size variability. In addition, a total of 20 well-silicified body scales were measured from both European and North American populations to statistically analyse the following morphological traits: i) scale length, ii) scale width, iii) the average number of pores enclosed in the mesh of the secondary layer (measured by averaging a total of 20 randomly selected meshes). In addition, we measured the length of well-developed bristles (12 and 16 bristles measured on European and North American populations, respectively). All measurements were performed using ImageJ 1.46 r (RASBAND 1997) and visualized in Rv.4.4.0 (R Core Team, 2021) using the packages "ggplot2" and "ggsignif". The differences between groups were tested using a two-sample t-test. The strains CA 33D and CZ 34M were further washed by repeated centrifugation in distilled water, air dried on coverslips, attached to aluminium stubs with double-sided adhesive carbon tape, coated with platinum and palladium (4:1) for 95s using a Bal-Tec SCD 050 sputter coater (Bal-Tec, Balzers, Lichtenstein), and observed with a JEOL Field emission scanning electron microscope JSM-IT800 (JEOL Ltd., Tokyo, Japan).

For ITS rDNA genotyping, 100 μ l of the culture were centrifuged in PCR tubes (6000 rpm for 3 min), and 30 μ l of InstaGene matrix (Bio–Rad Laboratories, Hercules, CA, USA) were added to the pellet. The solution was vortexed

Fottea, Olomouc, 25(2): 169–182, 2025 DOI: 10.5507/fot.2025.008

for 10 s, incubated at 56 °C for 30 min, and heated at 99 °C for 8 min. After vortexing a second time, the tubes were centrifuged at 12,000 rpm for 2 min, and the supernatant was directly used as a PCR template. The amplification of ITS rDNA was performed as described in Kynčlová et al. (2010), using the primers Kn1.1 (5'-CAA GGT TTC CGTAGG TGA ACC-3'; WEE et al. 2001) and ITS4 (5'-TCC TCC GCT TAT TGATAT GC-3'; WHITE et al. 1990). The PCR products were purified and sequenced at Macrogen Inc. in Seoul, Korea. Four M. intermedia strains (CZ 34M, CZ 35C, CA 33B, CA 56G) and one comparative strain of M. galeiformis Nicholls (US 36D) were selected for further sequencing of additional loci. After harvesting approximately 300 µL of well-grown cultures, DNA was isolated using the DNeasy Blood & Tissue Kit (Quiagen, Venlo, The Netherlands). Next, DNA libraries were prepared using the xGenTM DNA Library Prep EZ UNI Kit, and sequenced on the Illumina NextSeq platform, with 150 bp paired-end reads. Sequenced reads were trimmed with trimmomatic v. 0.32, using Phred quality scores of 33. De novo assembly of plastid genomes was performed in GetOrganelle v. 1.7.7.0, using Mallomonas splendens (G.S.West) Playfair (NC 040135) and Synura uvella Ehrenberg (NC 040134) chloroplast genome sequences as a seed. The genomes were assembled using default settings, with different k-mer sizes (21, 45, 65, 85, and 105). Gene prediction was carried out in MFannot (http://megasun.bch.umontreal.ca/apps/mfannot/) and the plastid LSU rDNA, psaA, and rbcL genes were subtracted for the phylogenetic analysis. Nuclear SSU and LSU rDNA genes were extracted from the trimmed sequenced reads by bwa v. 0.7.3a (Li & Durbin 2009) using a local alignment of rDNA sequences. The list of sequenced strains, including GenBank accessions, are given in Supplementary Table 1.

ITS rDNA sequences were aligned manually and investigated by performing a network analysis in Haplotype Viewer software (SALZBURGER et al. 2011). The sequences of nu-SSU rDNA, nu-LSU rDNA, pt-LSU rDNA, pt-rbcL, and pt-psaA were supplemented by sequences deposited in the GenBank database, and aligned using MAFFT v. 7 under the Q-INS-I strategy (KATOH et al. 2019). The loci were concatenated, yielding a robust alignment of 9,941 bases, 62 Mallomonas strains, and four outgroup taxa. Prior to performing the concatenated phylogenetic analysis, maximum likelihood (ML) analyses were performed separately for each locus in RAxML 8.1.20 (STAMATAKIS 2014) to verify there were no obvious topological incongruencies among the loci. The Bayesian evolutionary analysis was performed to infer a phylogeny and simultaneously estimate branch divergence times, using the program BEAST v. 2.5.0 (BOUCKAERT et al. 2019). The analysis was performed on a concatenated dataset divided into nine partitions (ribosomal genes, and codon-partitioned protein-encoded genes). For each partition, the most appropriate substitution model was estimated using the Bayesian information criterion (BIC) as implemented in jModelTest 2.1.4 (DARRIBA et al. 2012). This BIC-based model selection procedure selected the following models: (i) GTR + Γ + I for the nu–SSU, nu–LSU, and pt–LSU rDNA, and the first codon positions of the pt-rbcL gene, (ii) GTR + Γ for the first and third codon positions of the pt–psaA gene and the third codon positions of the pt-rbcL gene, (iii) GTR + I for the second codon positions of the pt–psaA gene, and (iv) JC for the second codon positions of the pt rbcL gene.

Several BEAST analyses were conducted to test for the effect of setting different priors for temporal constraints used to calibrate the *Mallomonas* phylogeny. Calibration was based on the fossil scales found in lacustrine mudstones from the Giraffe and Wombat cores, respectively (SIVER 2023). Either

8 or 12 temporal constraints were used. In the 8-calibration strategy, the constraints were used to calibrate only the clades containing several extant species and a fossil morphologically belonging to the given group of species. These constraints include (i) the split between M. alpina Pascher et Ruttner and M. elongata Reverdin (series Alpinae; Giraffe core), (ii) the lineage comprising M. corymbosa Asmund, M. poseidonii (Siver) Knotek et Škaloud, M. portae-ferreae Péterfi et Asmund and M. tonsurata Teiling (series Tonsuratae; Giraffe core), (iii) the lineage of M. bangladeshica (Takahashi et Hayakawa) Siver et Wolfe, M. peronoides (Harris) Momeu et Péterfi and M. ceylanica Dürrschmidt et Cronberg (fossilized M. bangladeshica; Giraffe core), (iv) the lineage comprising M. asmundiae Nicholls, M. striata Asmund and M. striata var. serrata Harris et Bradley (fossilized M. asmundiae; Giraffe core), (v) the lineage comprising M. doignonii Bourrelly, M. elevata H.S.Kim, M. eoa Takahashi, M. favosa Nicholls, M. foveata (Dürrschmidt) Gusev, M. munda (Asmund, Cronberg et Dürrschmidt) Němcová, M. schwemmlei Glenk and M. torquata Asmund et Cronberg (section Torquatae; Giraffe core), (vi) the lineage comprising M. cuspis Jeong, J.I.Kim, Jo, H.S.Kim, Siver et Shin, M. heterospina Lund and M. oviformis Nygaard (section Heterospinae and fossilized *M. oviformis*; Giraffe core), (vii) the lineage comprising M. adamas Harris et Bradley, M. pseudobronchartiana Gusev, Siver et Shin and M. splendens (G.S.West) Playfair (section Quadratae; Wombat core), and (viii) the lineage of M. caudata Iwanoff, M. hexareticulata Jo, Shin, H.S.Kim, Siver et Andersen, M. lacuna Jo, Shin, H.S.Kim, Siver et Andersen, M. matvienkoae Asmund et Kristiansen, M. pseudomatvienkoae Jo, Shin, H.S.Kim, Siver et Andersen and M. sorohexareticulata Jo, Shin, H.S.Kim, Siver et Andersen (section Planae; Wombat core). In the 12-calibration strategy, four additional calibrations were included, based on the occurrence of putative ancestor of a single extant species. These constraints included (ix) the parent node of M. intermedia (Giraffe core), (x) the parent node of M. lelymene Harris et Bradley (Giraffe core), (xi) the parent node of M. heterospina (section Heterospinae; Giraffe core), and (xii) the parent node of *M. insignis* Penard (Wombat core). Four strategies were applied to specify a distribution for the constraints. We set either (a) a log-normal distribution with a mean of 15, a standard deviation of 0.6, and an offset of either 48 (Giraffe core) or 82 Mya (Wombat core), (b) a log-normal distribution with a mean of 5, a standard deviation of 1, and the same offset as described above, (c) a uniform distribution with lower and upper limits of either 48–148 (Giraffe core) or 82–182 Mya (Wombat core), and (d) a uniform distribution as described above, further calibrating the age of the genus Mallomonas by setting a uniform distribution with lower and upper limits of 150-200 Mya following the Ochrophyta time-calibrated phylogenetic analysis published by Brown & SORHANNUS (2010). For all analyses, we linked both clock and tree models among the partitions. A lognormal relaxed clock model and a birth-death diversification process were used as a prior on the distribution of node heights. Three Markov Chain Monte Carlo (MCMC) analyses were run for 200 million generations, sampling every 5,000 generations. The analyses were run in the Czech Academic National Grid Infrastructure MetaCentrum, splitting the individual loci partitions onto multiple CPU resources by using the -beagle_order command-line option. After the diagnosis for convergence using Tracer 1.6, the tree files were merged using the burn-in set to 50 million generations and the Maximum Clade Credibility tree was summarized in TreeAnnotator.

Table 1. List of *Mallomonas* samples observed in this study, along with detailed characteristics of localities and a number of isolated strains per each locality.

Code of locality	Locality	Number of isolated strains	Sampling date	GPS coordinations	Temp.	pН	Cond. (μS.cm ⁻¹)
M. interm	edia						
BE 06	Natuurreservaat Tommelen – bomb crater, Belgium	3	11.04.2024	50.9345119, 5.30939440	13	7.8	71
CZ 08	Alluvial pool Drnků near Lužnice River, Czechia	2	12.03.2020	48.8527617, 14.9087042	10.5	8.2	228
CZ 13	Alluvial pool 192 near Lužnice River, Czechia	1	13.03.2020	48.8592340, 14.8977150	9.1	7.1	186
CZ 31	Alluvial pool Drnků near Lužnice River, Czechia	2	27.04.2020	48.8527617, 14.9087042	13.6	6.9	238
CZ 34	Oxbow lake near Lužnice River, Such- dol, Czechia	7	27.04.2020	48.9088967, 14.8907903	13.8	7.1	207
CZ 35	Canal Zlatá stoka, Czechia	7	27.04.2020	48.9518128, 14.8681525	12.2	7.7	288
CZ 85	Forest pond, Czechia	_	09.10.2020	49.0000575, 14.8129264	11.3	6.5	102
CZ 103	Wetland Na Plachtě, Czechia	1	26.10.2020	50.1882772, 15.8617333	11.4	6.9	60
CZ 110	Oxbow lake near Lužnice River, Such- dol, Czechia	5	30.10.2020	48.8488272, 13.9246825	7.5	6.7	79
CZ 186	Alluvial pool Drnků near Lužnice River, Czechia	2	14.02.2022	48.8527617, 14.9087042	_	=	-
CZ 204	Vlčí Jámy, Czechia	5	28.10.2022	48.9194972, 13.7798108	7.9	6.7	128
CZ 205	River Řasnice, Czechia	1	28.10.2022	48.9090719, 13.7459431	7.5	6.7	93
EE 08	Tänassilma jögi, Estonia	2	10.05.2023	58.3957578, 25.7031581	13.2	8.1	575
EE 12	Halliste jögi, Estonia	3	11.05.2023	58.3631903, 25.0601917	14.6	7.6	431
EE 13	Risti jögi, Estonia	-	11.05.2023	58.3661578, 25.0616769	15.4	7.7	442
HU 02	Risztics parlag, Hungary	1	15.04.2022	47.7058658, 19.0426764	10.8	6.8	173
HU 28	Jávor–tó (Rekketyés- tó), Hungary	-	17.03.2024	47.7139606, 19.0192092	15.9	6.8	133
HU 36	Csíkos–tó, Hungary	2	19.03.2024	47.7210558, 19.0720525	7.1	7.3	111
HU 48	Ilona–tó, Hungary	1	18.03.2025	47.7134056, 19.0402217	1.8	6.4	161
HU 49	unnamed pond, Hungary	2	18.03.2025	47.7154150, 19.0370917	3	7	59
HU 50	unnamed pond, Hungary	-	18.03.2025	47.7103358, 19.0389214	2.1	6.9	110
HU 51	Mély mocsár, Hun- gary	3	18.03.2025	47.7075106, 19.0403472	2.5	6.1	148

Table 1 Cont.

Vértes-mezo, Hungary	_	19.03.2025	47.7411522, 19.0440444	5.3	7.3	88
Csíkos-tó, Hungary	6	20.03.2025	47.7211572, 19.0720264	6.4	7.5	103
Unnamed pond, Netherlands	8	12.11.2021	51.6048244, 5.18174860	9.1	6.8	132
Meerbaansblaak, Netherlands	1	14.11.2021	51.3282606, 5.80269860	8.4	5.2	66
Alblas, Netherlands	3	16.11.2021	51.8605725, 4.66094250	9	7.7	641
Kars mosse, Sweden	1	31.05.2021	56.2939022, 12.4876758	20.7	6.8	247
Rönne å River, Sweden	1	31.05.2021	56.1203081, 13.1293250	18.7	7.1	259
dia sp. nov.						
Unnamed lake near Hubbles Lake Road, Alberta, Canada	7	04.10.2022	53.5753856, -114.0993108	14.9	7.9	131
Unnamed lake at Kathmarcam Estate, Alberta, Canada	3	06.10.2022	53.6078061, -114.0860567	14	8	109
Dog leg lake, Alberta, Canada	_	06.10.2022	53.6162069, -114.0673553	7.7	7.6	164
Canal at Veterans Memorial Hwy, Alberta, Canada	1	08.10.2022	54.1726047, -112.0287122	10.6	7.5	383
Grasshopper Lake, Florida, USA	_	10.10.2022	29.1344517, -81.6198028	30.6	4	40
Penner Lake, Florida, USA	-	11.10.2022	29.4908386, -81.8218833	29	5.1	42
	gary Csíkos-tó, Hungary Unnamed pond, Netherlands Meerbaansblaak, Netherlands Alblas, Netherlands Kars mosse, Sweden Rönne å River, Sweden Rönne å River, Sweden Unnamed lake near Hubbles Lake Road, Alberta, Canada Unnamed lake at Kathmarcam Estate, Alberta, Canada Dog leg lake, Alberta, Canada Canal at Veterans Memorial Hwy, Alberta, Canada Grasshopper Lake, Florida, USA Penner Lake, Flo-	gary Csíkos-tó, Hungary 6 Unnamed pond, Netherlands Meerbaansblaak, Netherlands Alblas, Netherlands 3 Kars mosse, Sweden 1 Rönne å River, Sweden 1 Rönne å River, Sweden 1 Unnamed lake near Hubbles Lake Road, Alberta, Canada Unnamed lake at Kathmarcam Estate, Alberta, Canada Dog leg lake, Alberta, Canada Canal at Veterans Memorial Hwy, Alberta, Canada Grasshopper Lake, Florida, USA Penner Lake, Flo-	gary Csíkos-tó, Hungary 6 20.03.2025 Unnamed pond, 8 12.11.2021 Netherlands Meerbaansblaak, 1 14.11.2021 Netherlands Alblas, Netherlands 3 16.11.2021 Kars mosse, Sweden 1 31.05.2021 Rönne å River, Sweden 1 31.05.2021 den dia sp. nov. Unnamed lake near 7 04.10.2022 Hubbles Lake Road, Alberta, Canada Unnamed lake at 3 06.10.2022 Kathmarcam Estate, Alberta, Canada Dog leg lake, Alberta, Canada Canal at Veterans 1 08.10.2022 Memorial Hwy, Alberta, Canada Grasshopper Lake, Florida, USA Penner Lake, Florida, USA	gary Csíkos-tó, Hungary 6 20.03.2025 47.7211572, 19.0720264 Unnamed pond, Netherlands 8 12.11.2021 51.6048244, 5.18174860 Meerbaansblaak, Netherlands 1 14.11.2021 51.3282606, 5.80269860 Alblas, Netherlands 3 16.11.2021 51.8605725, 4.66094250 Kars mosse, Sweden 1 31.05.2021 56.2939022, 12.4876758 Rönne å River, Sweden 1 31.05.2021 56.1203081, 13.1293250 dia sp. nov. Unnamed lake near 7 04.10.2022 53.5753856, -114.0993108 Hubbles Lake Road, Alberta, Canada 06.10.2022 53.6078061, -114.0860567 Kathmarcam Estate, Alberta, Canada 06.10.2022 53.6162069, -114.0673553 Dog leg lake, Alberta, Canada 06.10.2022 54.1726047, -112.0287122 Memorial Hwy, Alberta, Canada 08.10.2022 54.1726047, -112.0287122 Memorial Hwy, Alberta, Canada 10.10.2022 29.1344517, -81.6198028 Penner Lake, Flo- 11.10.2022 29.4908386, -81.8218833	gary Csíkos-tó, Hungary 6 20.03.2025 47.7211572, 19.0720264 6.4 Unnamed pond, Netherlands Meerbaansblaak, Netherlands Alblas, Netherlands Alblas, Netherlands 3 16.11.2021 51.3282606, 5.80269860 8.4 Kars mosse, Sweden 1 31.05.2021 56.2939022, 12.4876758 20.7 Rönne å River, Sweden 1 31.05.2021 56.1203081, 13.1293250 18.7 dia sp. nov. Unnamed lake near Hubbles Lake Road, Alberta, Canada Unnamed lake at Kathmarcam Estate, Alberta, Canada Dog leg lake, Alberta, Canada Canal at Veterans Memorial Hwy, Alberta, Canada Grasshopper Lake, Florida, USA Penner Lake, Flo- 11.10.2022 29.4908386, -81.8218833 29	gary Csíkos-tó, Hungary 6 20.03.2025 47.7211572, 19.0720264 6.4 7.5 Unnamed pond, Netherlands 8 12.11.2021 51.6048244, 5.18174860 9.1 6.8 Meerbaansblaak, Netherlands 1 14.11.2021 51.3282606, 5.80269860 8.4 5.2 Alblas, Netherlands 3 16.11.2021 51.8605725, 4.66094250 9 7.7 Kars mosse, Sweden 1 31.05.2021 56.2939022, 12.4876758 20.7 6.8 Rönne å River, Sweden 1 31.05.2021 56.1203081, 13.1293250 18.7 7.1 dia sp. nov. Unnamed lake near Hubbles Lake Road, Alberta, Canada 04.10.2022 53.5753856, -114.0993108 14.9 7.9 Hubbles Lake Road, Alberta, Canada 06.10.2022 53.6078061, -114.0860567 14 8 Lonamed lake at Kathmarcam Estate, Alberta, Canada 06.10.2022 53.6162069, -114.0673553 7.7 7.6 Log leg lake, Alberta, Canada 08.10.2022 54.1726047, -112.0287122 10.6 7.5 Memorial Hwy, Alberta, Canada 08.10.2022 54.1726047,

RESULTS

A total of 81 strains morphologically corresponding to the circumscription of *M. intermedia* were isolated from 27 freshwaters localities in Belgium, Czechia, Estonia, Hungary, the Netherlands, Sweden, and Alberta, Canada (Table 1). In addition, we recovered *M. intermedia* silica scales in four localities in the Czechia, Estonia, and Florida, USA, from which we were unsuccessful in establishing living cultures.

ITS rDNA barcoding of cultured strains revealed the existence of two distinct genotypes with a strict geographical pattern, differing by 12 nucleotide substitutions (Fig. 1). The most abundant genotype, here referred to as *M. intermedia*, was isolated from European localities, while the second genotype, here referred to as *M. retimedia*, sp. nov., was represented by 11 Canadian isolates only.

A total of eight Bayesian evolutionary analyses of the multigene dataset were performed, differing by setting various temporal constraints used to calibrate the Mallomonas phylogeny (see Materials and Methods). All analyses resulted in identical topologies; however, they differed considerably by the estimated age of the genus Mallomonas. When allowed for older age in the distribution setting of clades comprising fossil taxa (a lognormal distribution with a mean of 15 or a uniform distribution), the Mallomonas age was estimated to be 350-570 Mya. By applying a temporal constraint for the genus Mallomonas or by using a lognormal distribution that gives high probability of the origin of clades just a few million years prior to the fossil discovery, more reliable Mallomonas ages were estimated, ranging from 195 to 215 Mya (Fig. 2). The analyses recovered a close relationship between M. intermedia and M. retimedia, sp. nov., which diverged approximately 7.9 (\pm 6.4) or 8.4 (\pm 7.3) million years ago (by using a uniform or lognormal distribution, respectively). These two species form part of a broader clade within the section Mallomonas that encompasses M. corymbosa, M. poseidonii, M. portaeferreae, and M. tonsurata (Fig. 2).

Mallomonas intermedia cells were ovoid to

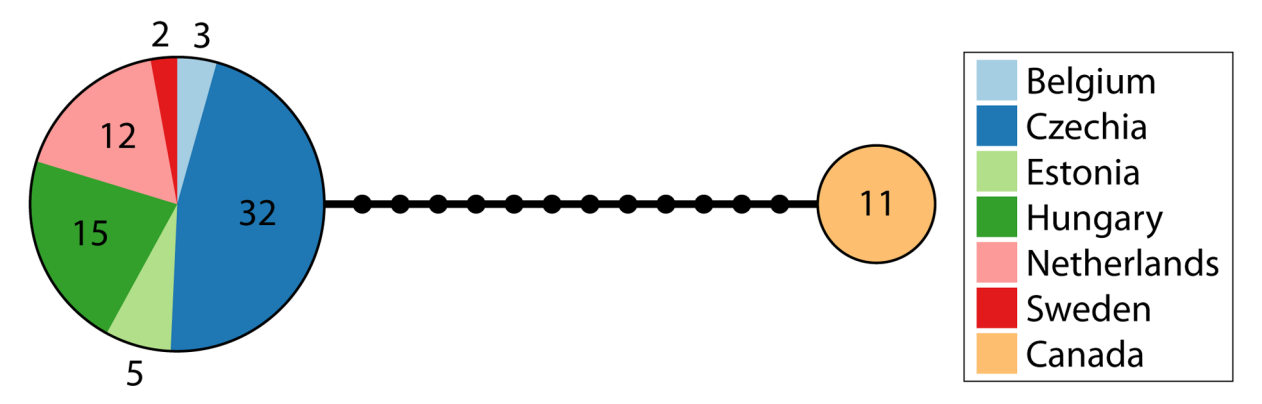


Fig. 1. ITS rDNA haplotype network showing the genetic differentiation between the European and North American M. intermedia strains.

ellipsoidal, 17–25 μm long and 12–16 μm wide. The cells were encased in siliceous scales and formed a number of bristles, which covered the entire cell except for the very posterior end (Figs 3A,B). The body scales, usually integrated with a well-developed dome, ranged from 4.5–6.9 μm in length and 3.1–4.1 μm in width. The base plate was covered with small, evenly spaced pores that form curved transverse rows along the distal portion of the shield (Fig. 3C). Pores were randomly distributed at the proximal end of the scale and formed a patch of differently arranged small pores at the V-rib base (Fig. 3D). The secondary reticulation was generally weakly developed, and when richly developed, it usually surrounded one, rarely two pores of the basal plate (Figs 3E,F). Areas resembling holes, where no pores were present in the basal plate, appeared irregularly (Fig. 3E). The dome was prominent, with either a series of thin and parallel ribs or a single rib (Figs 3D-F). A single, prominent transverse rib was present on the shield at the base of the dome. Smaller scales without domes and lacking the transverse shield rib were also observed (Fig. 3G). Two types of bristles were identified, varying in length depending on their position on the cell. In the field, bristles measured 15–35 μm, while in culture, they were 13–20 μm long. Shorter bristles had a pointed apex and prominent serration along their entire length (Fig. 3H), whereas longer bristles terminated with a lance-shaped apex and were mostly smooth (Fig. 3I).

Mallomonas retimedia sp. nov. cells were similarly ovoid to ellipsoidal, measuring 19–27 μm in length and 12–16 μm width. The cells were surrounded by siliceous scales and formed bristles covering the entire cell except for the very posterior end (Figs 4A,B). The body scales, usually possessing a well–developed dome, ranged from 4.5–6.3 μm in length and 2.9–4.1 μm in width. The base plate was covered with small, evenly spaced pores that formed curved transverse rows along the distal portion of the shield (Fig. 4C). Pores were randomly arranged at the proximal end of the scale and formed a patch of differently arranged small pores at the V–rib base (Figs 4D,E). The secondary reticulation was usually richly developed, encircling mostly 3–4 pores of the basal plate (Figs 4C–E). Areas resembling holes, where no pores

were present in the basal plate, appeared irregularly (Fig. 4F). The dome was large, usually without or with a single indistinct rib (Figs 4C–F). A single, prominent transverse rib was present on the shield at the base of the dome. Smaller scales without domes and lacking the transverse shield rib were also observed (Fig. 4G). Two types of bristles were identified, varying in length depending on their position on the cell. In the field, bristles measured 15–28 μ m long, while in culture they were 14–20 μ m long. Shorter bristles had a pointed apex and prominent serration along their entire length (Fig. 4H), whereas longer bristles ended with a lance–shaped apex and were mostly smooth (Fig. 4I).

Comparative analyses of measured morphological traits revealed no significant differences between *M. intermedia* and *M. retimedia*, sp. nov. in terms of scale and bristle dimensions (Fig. 5), though *M. retimedia*, sp. nov. exhibited slightly longer scales and shorter lance—terminated bristles. The most notable difference between the species was in the number of pores enclosed in the mesh formed on the siliceous scales (Fig. 5D). While the secondary reticulation in *M. intermedia* typically surrounded only one pore of the basal plate, the secondary layer meshes of *M. retimedia*, sp. nov. encircled an average of 3.1 pores.

DISCUSSION

Taxonomic consequences

Our morphological observations of North American *M. intermedia* populations correspond well to those reported by Siver et al. (2019) from Dufurrena Pond 19 in the Virgin Valley region of northern Nevada. Interestingly, the cells we observed were considerably shorter than those observed in northern Nevada (19–27 µm versus 31–42 µm). It is very likely that this difference is mainly due to the fact that we measured cells in culture, where size changes can occur, for example as a result of different temperatures (ATKINSON et al. 2003; Řezáčová–ŠKALOUDOVÁ et al. 2010; PICHRTOVÁ & NĚMCOVÁ 2011) or the absence of grazing pressure (BRANCO et al. 2020).

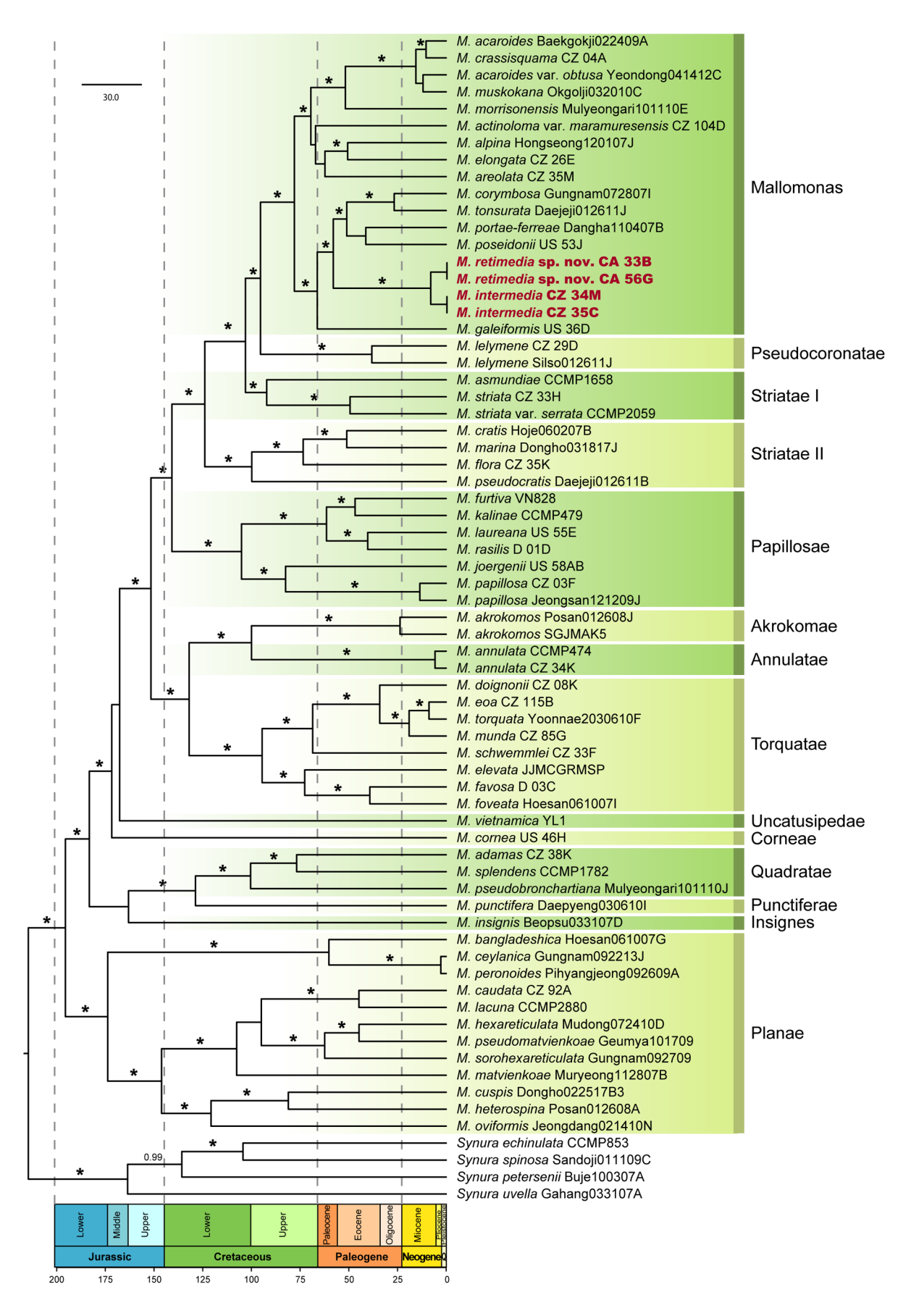


Fig. 2. Time–calibrated phylogeny of the genus *Mallomonas* based on concatenated nu–SSU rDNA, nu–LSU rDNA, pt–*rbc*L, pt–*psa*A, and pt–LSU rDNA sequences. Values at nodes indicate statistical support estimated by Bayesian posterior probability. Asterisks mark nodes with the highest statistical support (1.00). Time axis is in million years ago (Mya), along with chronological dating of geologic intervals. Scale bar represents the expected number of substitutions per site.

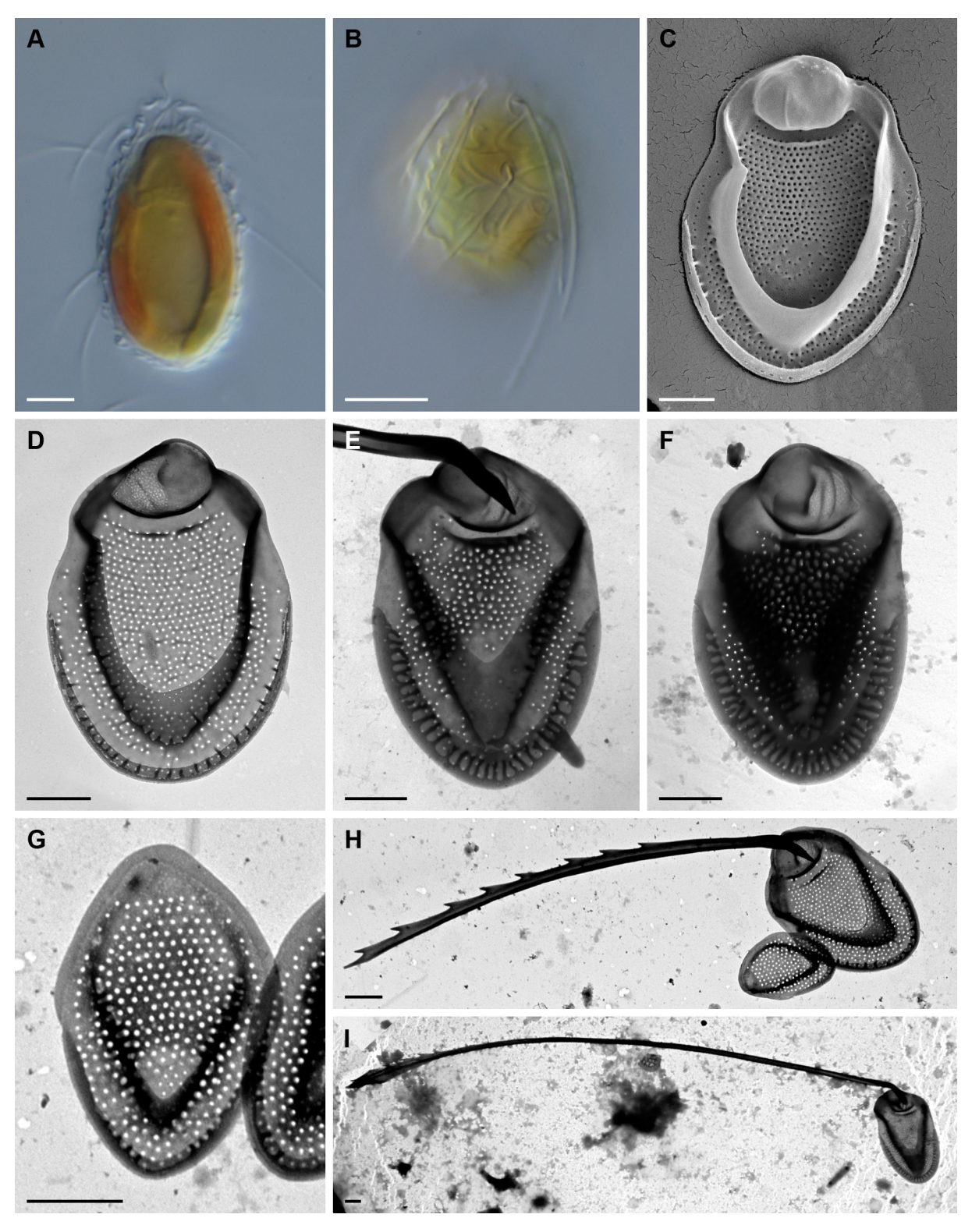


Fig. 3. *Mallomonas intermedia*: (A–B) Whole cell with visible scales and bristles; (C–D) body scales of cultured strains; (E–F) body scales from plankton samples; (G) dome–less rear scale; (H) short bristle with a pointed end; (I) long bristle with a lance–shaped apex. Images taken by (A–B) LM, (C) SEM, (D–I) TEM. Scale bars 10 μm (A–B), 1 μm (C–I).

On the other hand, scale and bristle morphology were virtually identical, especially in the terms of secondary layer forming a reticulation encircling several pores of the basal plate. It is worth mentioning that the scales of Nevada population were longer and had more ribs on the dome than cells from our cultures from Alberta, Canada. However, we do not consider the presence and number of ribs on the dome to be an important taxonomic characteristic, as it is known to be variable on other species of the genus *Mallomonas* (KRISTIANSEN

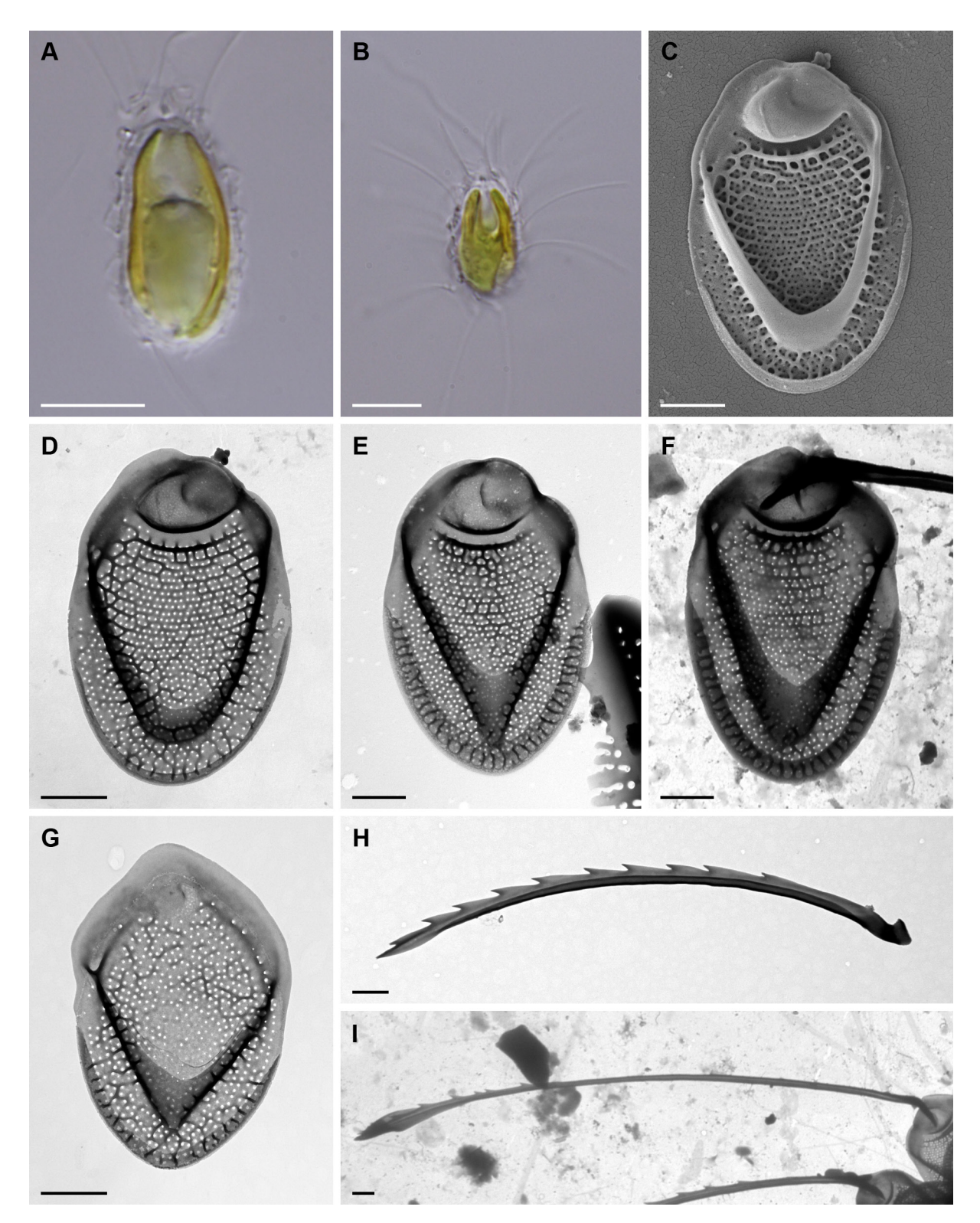


Fig. 4. *Mallomonas retimedia*, sp. nov: (A–B) whole cell with visible scales and bristles; (C–D) body scales of cultured strains; (E–F) body scales from plankton samples; (G) dome–less rear scale; (H) short bristle with a pointed end; (I) long bristle with a lance–shaped apex. Images taken by (A–B) LM, (C) SEM, (D–I) TEM. Scalebars 10 μm (A–B), 1 μm (C–I).

2002), and it is likely related to growth and environmental conditions, especially silica availability (SIVER et al. 2019). Accordingly, we conclude that the Nevada population is conspecific with our observed populations in Canada and the USA and forms an endemic lineage

for North America.

Considering the presented genetic and morphological differences between European and North American populations, we conclude they represent distinct species that originated in the Miocene epoch, approximately 8

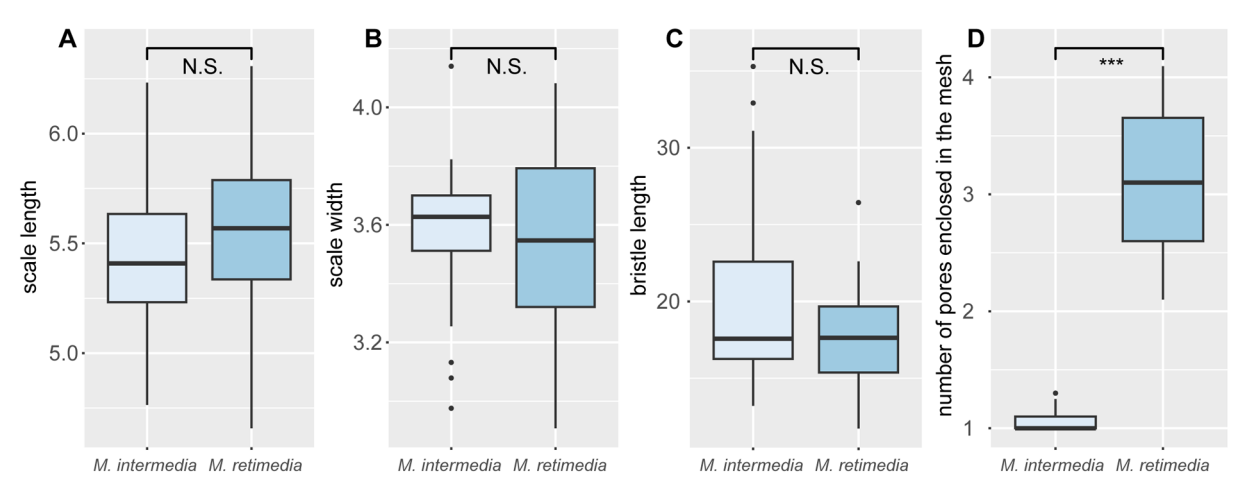


Fig. 5. Boxplots of four measured morphological traits in M. intermedia and M. retimedia, sp. nov: (A) scale length; (B) scale width; (C) bristle length; (D) number of pores enclosed in the mesh of a secondary layer in silica scales. The results of two–sample t–tests are given at the top of the graphs: N.S. = not significant, *** = p-value < 0.001).

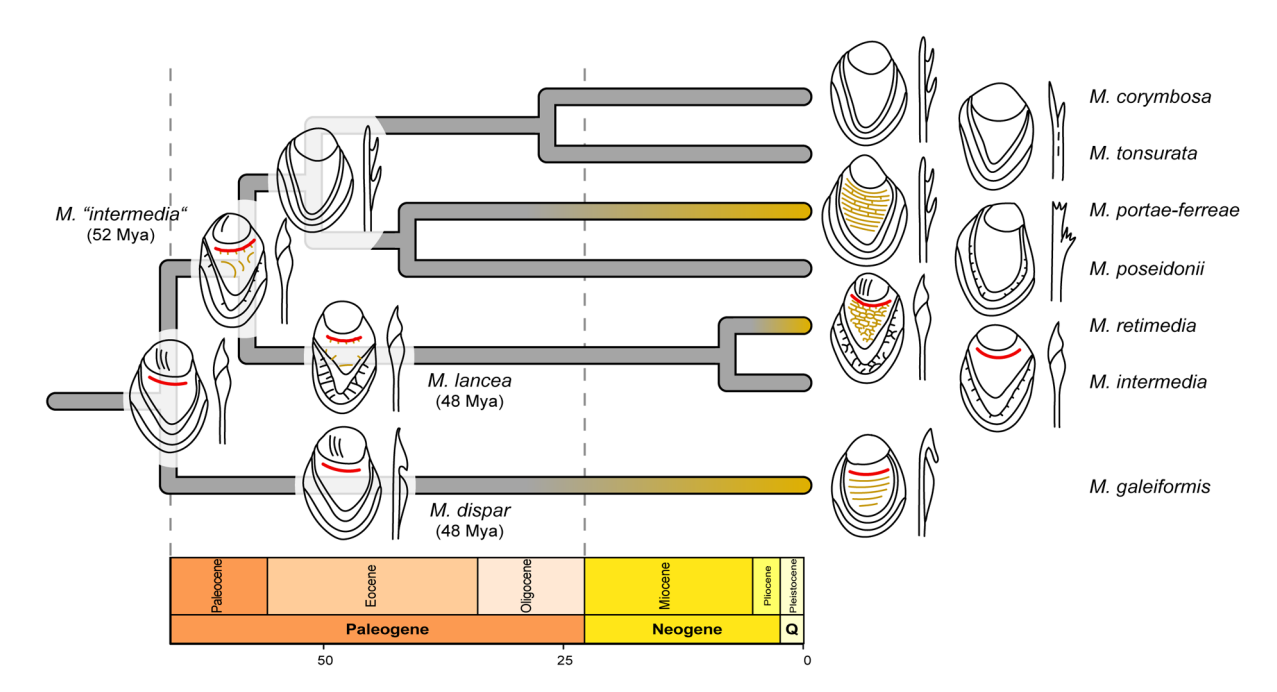


Fig. 6. A proposed morphological evolution of dome-bearing silica scales and bristle tips in the *Mallomonas intermedia* group, based on the combination of fossil evidence and inferred time-calibrated phylogeny. The formation of a distinct transverse rib is illustrated in red. Other ribs and reticulations present on the shield of silica scales are shown in gold. The proposed evolution of parallel ribs on the siliceous scales is illustrated by gold coloration of branches. Time axis is in million years ago (Mya), along with chronological dating of geologic intervals.

million years ago. The most prominent discriminating feature is the pattern of secondary reticulation on the shield of siliceous scales. If the secondary reticulation is well developed, then the lineages can undoubtedly be distinguished by the different mesh size in reticulation (Fig. 5D). Generally, much more pronounced secondary reticulation was found in scales from plankton samples than in those from cultures (compare Fig. 3D and Figs 3E–F). Accordingly, given the possible occurrence of different amounts of silicon in nature, it can sometimes be difficult to distinguish between the two lineages due to the incomplete formation of the secondary layer. Indeed, some less silicified scales from European populations

may exhibit fine reticulation (Figs 3C,D). However, this never forms a closed network surrounding several pores as seen in North American populations (Figs 4C–F). *M. intermedia* was described by Kisselev (1931) from a polluted pond near Peterhof, Russia. Despite the fact that the description is based on light microscopic observations without a detailed description of the ultrastructure of the siliceous scales, it is very consistent with our observed morphology, particularly in the shape of the cell, the shape and organization of the scales, and the morphology of long bristles ending with a lance—shaped apex. Interestingly, the length of our cells measured in the culture is again much smaller than reported by Kisselev (1931) (17–25

Fottea, Olomouc, 25(2): 169–182, 2025 DOI: 10.5507/fot.2025.008

 μ m versus 31–42 μ m), which confirms our hypothesis of cell shortening in culture. Since we have not detected a genetically distinct North American population in any of the European localities we have examined, we believe that the European lineage corresponds to the species of M. intermedia as circumscribed by Kisselev (1931). Prior to the formal description of the North American lineage as a new species, it is necessary to delimit it from all previously described species, primarily focusing on those described from the North American continent. We identified two Mallomonas species described from the USA without a description of the ultrastructure of the siliceous scales. M. litomesa Stokes was described by Stokes (1885) from marsh water in New Jersey. Morphologically, this species resembles M. teilingii Conrad by forming fusiform cells with bristles restricted to the ends. The second species, M. urnaformis Prescott, was described by PRESCOTT (1944) from a lake in Wisconsin. This species forms elliptic cells with a neck and is covered by rectangular scales in regular transverse rows, resembling species belonging to the section Punctiferae, and may be conspecific with either M. nieringii Siver or M. connensis Siver & Marsicano, both representing North American endemic species. Considering the silica scale morphology, the North American lineage is similar to M. portae-ferreae var. reticulata Gretz, Sommerfeld & Wujek described from a lake in Arizona (GRETZ et al. 1985). This taxon has a somewhat similar reticulation on the scale shield, but lacks a distinct transverse rib running parallel to the base of the dome. In addition, three *M. intermedia* varieties were described in the past: var. gesticulans Péterfi (HARRIS 1953), var. soleata (Harris) Harris et Bradley in ASMUND (1959), and var. saliceaensis Péterfi et Momeu (Péterfi & Momeu 1977). The varieties were characterized by differences in bristle and cyst morphology, and in the presence of domes in body scales. Since all these varieties were described based on observations of European samples, they cannot represent North American populations. In addition, the descriptions of the two latter mentioned varieties were accompanied by the ultrastructure of their silicified scales, clearly indicating that they belong to the species M. intermedia. Consequently, because the North American lineage is not identical to any previously described Mallomonas species, we propose that it represents the new species M. retimedia, sp. nov. for which we propose a description here.

Mallomonas retimedia sp. nov. (Fig. 4)

Description: Cells are ovoid to ellipsoidal, 19–27 μm long and 12–16 μm wide, covered with tripartite scales. Body scales are oval, 4.5–6.3 μm long and 2.9–4.1 μm wide, with a dome and a well–developed V–rib. The V–rib arms are long, curved, and continuous with the anterior submarginal ribs, terminating on the dome sides. The dome is large, smooth or with a single indistinct rib. A distinct transverse rib runs parallel to the base of the

dome, formed anteriorly on the shield. The base plate has small, evenly spaced pores forming curved transverse rows, with irregularly scattered areas without pores. Pores are randomly arranged at the proximal end. The secondary layer has richly developed reticulation, with meshes usually encircling 3–4 pores. The reticulation is also developed along the V–rib and posterior flanges. Anterior flanges are smooth. Rear scales are smaller, and lack the dome and transverse shield rib. Bristles cover the cell except at the posterior end, with two types. Shorter bristles (up to 18 μm) with a pointed apex and prominent serration are usually formed anteriorly. Longer bristles (up to 28 μm) have a lance—shaped apex, are mostly smooth, and serrated at the ends.

Holotype: Portion of a single gathering of cells on SEM stub, deposited at the Culture Collection of Algae of the Charles University in Prague (CAUP) as the item TYPE–CA 33D. Fig. 4C illustrates a representative scale from the holotype specimen.

Type locality: Unnamed lake near Hubbles Lake Road, Alberta, Canada, 53.5753856, –114.0993108. Collected on 4th October 2022 by P. Škaloud and M. Pusztai.

Etymology: The species name "retimedia" is derived from Latin, where "reti—" refers to a net—like structure and "—media" suggests an intermediate form. This name highlights the morphological similarity to *M. intermedia*, emphasizing its distinctive feature: a richly developed reticulation in the secondary layer of siliceous scales.

Distribution and ecology: Endemic to North America, it has been recorded in Canada (Alberta) and the USA (Florida, Nevada). It occurs in a wide range of freshwater bodies (lakes, ponds, canals) and environmental conditions (observed pH range: 4.0–8.0, conductivity range 40–383 μS. cm⁻¹).

Diversification and morphological evolution of *M. intermedia* and related species

M. intermedia and M. retimedia originated in the Miocene epoch approximately 8 million years ago. This period was characterized by significant changes in climate and geography, leading to the evolution and diversification of many plant and animal species (STRÖMBERG 2011; WERDELIN & LEWIS 2013). Both species belong to the Mallomonas of section Mallomonas, characterized by a shield that is smooth or has striation or reticulum. Three monophyletic groups of species may be identified within the section, sharing specific morphological features concerning their shield structure (Fig. 2). The first lineage, described as series Alpinae, comprises species with no secondary layer on the scale shield (M. alpina, M. areolata Nygaard, and M. elongata). The second lineage, comprising M. acaroides Zacharias, M. crassisquama (Asmund) Fott and M. muskokana (Nicholls) Siver, and described as series Mallomonas, is characterized by the shield marked with irregularly arranged struts or ribs, which may be joined into irregular, roughly hexagonal or circular meshes. Finally, the third lineage referred to

The ancestor of the Intermedia group probably

here as Intermedia group, comprised in our phylogeny by *M. corymbosa*, *M. galeiformis*, *M. portae–ferreae*, *M. poseidonii*, *M. tonsurata*, *M. intermedia* and *M. retimedia*, is characterized by the shield covered by a thick secondary layer, forming a reticulum with meshes encircling either one (in most species) or several pores (as in *M. retimedia* or *M. portae–ferreae*). In *M. galeiformis* and *M. portae–ferreae*, the reticulum forms regularly spaced ribs, in the latter species occasionally interconnected by cross ribs to form rectangular meshes.

Thanks to a unique collection of fossils, we have a unique opportunity to trace the morphological evolution of the Intermedia Group. A total of three fossils have been found with a distinct transverse rib running behind the base of the dome: M. dispar and M. lancea found in the Giraffe pipe dated to 48 Mya (SIVER et al. 2009), and the putative ancestor of M. intermedia found in the Horsefly core dated to 52 Mya (SIVER et al. 2019). SIVER (2023) suggested, based on a detailed analysis of the morphology of these fossils, that all of these species are possibly related to the modern species. M. dispar has been proposed as a probable ancestor of M. galeiformis, based on the similar size and shape of the scales, and also the demonstrated ability of M. galeiformis to produce only a single prominent rib situated near the base of the dome as in M. dispar (SIVER 1991, 2023). M. lancea was proposed as an ancestor of M. intermedia or M. corcontica (Kalina) Péterfi et Momeu based on scale and spine similarities (SIVER et al. 2015b). Finally, scales found in the Horsefly core were proposed as a direct ancestor of M. intermedia (SIVER et al. 2019).

By combining morphological observations of fossil species and temporal calibration based on genetic data, we can form an idea of the morphological evolution of the Intermedia group, focusing on both silica scales and bristles (Fig. 6). The ancestor of the lineage was probably without a thick secondary layer, but with a distinct transverse rib already formed, resembling M. dispar. A direct descendant of this ancestor is M. galeiformis, which developed additional ribs on the shield of the scale. It is likely that the anterior rib behind the dome was still present in the ancestor of the other six species, which resembled the "M. intermedia" scale found in the Horsefly core by SIVER et al. (2019). The rib evolutionarily disappeared in the ancestor of M. corymbosa, M. portae-ferreae, M. poseidonii and M. tonsurata, which very likely resembled M. corymbosa, i.e. by producing scales without the reticulation. In M. tonsurata, the secondary layer then thickened, while M. portae–ferreae formed a secondary reticulation with parallel ribs, not dissimilar to the reticulation in M. retimedia. The evolution towards the species M. intermedia and M. retimedia involved the formation of a reticulation on the shield, and the different patterns of this reticulation can be well illustrated in the fossil scales found 48 and 52 Mya. Approximately 8 Mya, speciation of the two recent species occurred, and in M. retimedia this reticulation was enhanced in the form

of interconnected meshes, whereas in *M. intermedia* it virtually disappeared.

had bristles terminated by a triangular-shaped tip referred to as the lance (SIVER 1991). The lance—tipped bristles were detected in both the "M. intermedia" and M. lancea fossil species, and were retained to the modern M. intermedia and M. retimedia (Fig. 6). However, we can trace several distinct changes in bristle formation during the evolution of other Intermedia group species. In the lineage leading to M. galeiformis, the bristle tip evolved into a distinctive helmet-tipped bristle with a deep and narrow groove and a folded membrane that covers part of the groove. SIVER et al. (2009) already hypothesized that helmet bristle tips might have evolved from the lance-tipped bristles by expanding a membrane along the ventral bristle surface to develop a cleft. Another distinct morphological change likely occurred in the ancestor of M. corymbosa, M. portae-ferreae, M. poseidonii and M. tonsurata, where the lance–tipped bristles developed into pointed, serrated bristles, which represent the most common bristle morphology in *Mallomonas*. The bristles in this group continued to evolve, with M. tonsurata developing simple bifurcated bristles, while M. poseidonii exhibited multifurcated bristle teeth. From the above, it is evident that the evolutionary rate of morphological changes varies in different parts of their silica scale case. While some structures, such as the V-rib, upturned rim, or dome shape, undergo almost no change for tens of millions of years (SIVER & WOLFE 2005; SIVER et al. 2009), the shield of the scales is in contrast the most morphologically plastic area, where the most rapid morphological changes take place. The most interesting structures in this respect are parallel ribs. These have been formed independently a total of three times in the Intermedia Group alone (in the species M. galeiformis, M. portae-ferreae, and M. retimedia), probably during the Miocene epoch. Parallel ribs have been created by parallel evolution in many other lineages of the genus (ČERTNEROVÁ et al. 2019) and thus it seems some adaptive function must be behind their repeated origin. However, recently published studies have shown that the ribs do probably not reduce dangerous UV radiation by light diffraction (Nemcová et al. 2024), nor do they improve the scale mechanical stability (KNOTEK & ŠKALOUD 2023). The ribs may play a role in the precise alignment and spacing of the scales on the cell surface or they could be responses to varying environmental pressures, such as predation or water currents (KNOTEK & ŠKALOUD 2023). However, further research is needed to trace the adaptive role, evolutionary significance, and formation rate of parallel rib formation on Mallomonas

ACKNOWLEDGEMENTS

siliceous scales.

We are very grateful to Kateřina Tučková and Veronika Kantnerová for their support with sampling. We also thank Peter A. Siver for valuable discussions concerning bristle evolution. The study was supported by the Czech Science Foundation, project No. 23–06881S.

Computational resources were provided by the e–INFRA CZ project (ID:90254), supported by the Ministry of Education, Youth and Sports of the Czech Republic. We acknowledge also the Charles University Viničná Microscopy Core Facility (RRID:SCR_026602), cofinanced by Czech–BioImaging large RI project LM2023050.

REFERENCES

- Annenkova, N.V.; Hansen, G.; Moestrup, Ø. & Rengefors, K. (2015): Recent radiation in a marine and freshwater dinoflagellate species flock. ISME Journal 9: 1821–1834.
- ASMUND, B. (1959): Electron microscope observations on *Mallomonas* species and remarks on their occurrence in some Danish ponds and lakes III. Dansk Botanisk Arkiv 18: 1–50.
- ATKINSON, D.; CIOTTI, B.J & MONTAGNES, D.J.S. (2003): Protists decrease in size linearly with temperature: ca. 2.5% °C-1.

 Proceedings. Biological Sciences 270: 2605–2611.
- Bendif, E.M.; Nevado, B.; Wong, E.L.Y; Hagino, K.; Probert, I.; Young, J.R.; Rickaby R.E.M. & Filatov, D.A. (2019): Repeated species radiations in the recent evolution of the key marine phytoplankton lineage Gephyrocapsa.

 Nature Communications 10: 1–9.
- BOUCKAERT, R.; VAUGHAN, T.G.; BARIDO—SOTTANI, J.; DUCHÊNE, S.; FOURMENT, M.; GAVRYUSHKINA, A. et al. (2019): BEAST 2.5: An advanced software platform for Bayesian evolutionary analysis. PLoS Computational Biology 15: e1006650.
- Branco, P.; Egas, M.; Hall, S.R. & Huisman, J. (2020): Why Do Phytoplankton Evolve Large Size in Response to Grazing? The American Naturalist195: E20–E37.
- Brown, J.W & Sorhannus, U. (2010): A Molecular Genetic Timescale for the Diversification of Autotrophic Stramenopiles (Ochrophyta): Substantive Underestimation of Putative Fossil Ages. PLoS ONE 5: e12759.
- CASTELEYN, G.; LELIAERT, F.; BACKELJAU, T.; DEBEER, A.E.; KOTAKI, Y.; RHODES, L.; LUNDHOLM, N.; SABBE, K. & VYVERMAN, W. (2010): Limits to gene flow in a cosmopolitan marine planktonic diatom. Proceedings of the National Academy of Sciences of the United States of America 107: 12952–12957.
- ČERTNEROVÁ, D.; ČERTNER, M. & ŠKALOUD, P. (2019): Molecular phylogeny and evolution of phenotype in silica—scaled chrysophyte genus *Mallomonas*. Journal of Phycology 55: 912–923.
- Gerstein, A.C. & Moore, J.S. (2011): Small is the new big: Assessing the population structure of microorganisms.
 – Molecular Ecology 20: 4385–4387.
- Gretz, M.R., Sommerfeld, M.R. & Wujek, D.E. (1985): Light and electron microscopical observations of *Mallomonas portae–ferreae* var. *reticulata* var. nov. (Chrysophyceae). Phycologia 24: 478–481.
- GUILLARD, R.R.L. & LORENZEN, C.J. (1972): Yellow–green algae with chlorophyllide C. J. Phycol. 8: 10–14.
- Harris, K. (1953): A contribution to our knowledge of *Mallomonas*.

 Botanical Journal of the Linnean Society 55: 88–102.
- HARRIS, K & BRADLEY, D.E. (1960): A taxonomic study of Mallomonas. – Journal of General Microbiology 22: 750–777.
- JADRNÁ, I. & ŠKALOUD, P. (2025): Exploring the factors shaping microscopic morphological traits: insights from the chrysophycean genus *Synura* (Stramenopiles). – European Journal of Phycology 60: 67–83.
- Jo, B.Y.; Shin, W.; Kim, H.S.; Siver, P.A. & Andersen, R.A. (2013): Phylogeny of the genus *Mallomonas* (Synurophyceae) and descriptions of five new species on the basis of

- morphological evidence. Phycologia 52: 266-278.
- KATOH, K.; ROZEWICKI, J. & YAMADA, K.D. (2019): MAFFT online service: multiple sequence alignment, interactive sequence choice and visualization. Briefings in Bioinformatics 20: 1160–1166.
- KISSELEW, J.A. (1931): Zur Morphologie einiger neuer und seltener Vertreter des pflanzlichen Mikroplankton. Archiv für Protistenkunde 3: 237–250.
- KNOLL, A. & KOTRC, B. (2015): Protistan Skeletons: A Geologic
 History of Evolution and Constraint. In: HAMM, C.
 (ed.): Evolution of Lightweight Structures. Biologically–
 Inspired Systems, vol 6. 1–16 pp., Springer, Dordrecht.
- KNOTEK, P. & ŠKALOUD, P. (2023): The effect of patterned structures on the mechanical resistance of microscopic silica scales. Fottea 23: 190–200.
- Kristiansen, J. (2002): The genus *Mallomonas* (Synurophyceae): a taxonomic survey based on the ultrastructure of silica scales and bristles. Opera Botanica 139: 1–218.
- Kristiansen, J. (2005): Golden Algae: A Biology of Chrysophytes.
 167 pp., A. R. G. Gantner Verlag, K.G., Ruggell.
- Kynčlová, A.; Škaloud, P. & Škaloudová, M. (2010): Unveiling hidden diversity in the *Synura petersenii* species complex (Synurophyceae, Heterokontophyta). Nova Hedwigia Beiheft 136: 283–298.
- Lebret, K.; Kritzberg, E.S.; Figueroa, R. & Rengefors, K. (2012): Genetic diversity within and genetic differentiation between blooms of a microalgal species. Environmental Microbiology 14: 2395–2404.
- LI, H. & DURBIN, R. (2009): Fast and Accurate Short Read Alignment with Burrows–Wheeler Transform. – Bioinformatics 25: 1754–1760.
- Logares, R.; Rengefors, K.; Kremp, A.; Shalchian-Tabrizi, K.; Boltovskoy, A.; Tengs, T.; Shurtleff, A. & Klaveness, D. (2007): Phenotypically different microalgal morphospecies with identical ribosomal DNA: a case of rapid adaptive evolution? Microbial Ecology 53: 549–561.
- Nemcova, Y.; Knotek, P.; Jadrná, I.; Černajová, I. & Škaloud, P. (2024): Nanopatterns on silica scales of *Mallomonas* (Chrysophyceae, Stramenopiles): Unraveling UV resistance potential and diverse response to UVA and UVB radiation. Journal of Phycology 60: 1256–1272.
- PÉTERFI, L.S & MOMEU, L. (1977): Observations on some *Mallomonas* species from Romania in light and transmission electron microscopes. Nova Hedwigia 28: 155–202.
- Pichrtová, M. & Němcová, Y. (2011): Effect of temperature on size and shape of silica scales in *Synura petersenii* and *Mallomonas tonsurata* (Stramenopiles). Hydrobiologia 673: 1–11.
- Postel, U.; Glemser, B.; Salazar Alekseyeva, K.; Eggers, S.L.; Groth, M.; Glöckner, G.; John, U.; Mock, T.; Klemm, K.; Valentin, K. & Beszteri, B. (2020): Adaptive divergence across Southern Ocean gradients in the pelagic diatom *Fragilariopsis kerguelensis*. Molecular Ecology 29: 4913–4924.
- Prescott, G.W. (1944): New Species and Varieties of Wisconsin Algae. Farlowia 1: 347–385.
- RASBAND, W.S. (1997–2018): ImageJ, U. S. National Institutes of Health. Bethesda, Maryland, USA. Available at: https://imagej.net/ij/.
- R Core Team (2021): R: A language and environment for statistical computing. R Foundation for Statistical Computing, Vienna, Austria. Available at: https://www.R-project.org/.
- Rengefors, K.; Logares, R. & Laybourn-Parry, J. (2012): Polar lakes may act as ecological islands to aquatic

- protists. Molecular Ecology 21: 3200-3209.
- Řezácová–Škaloudová, M.; Neustupa, J. & Němcová, Y. (2010): Effect of temperature on the variability of silicate structures in *Mallomonas kalinae* and *Synura curtispina* (Synurophyceae). Nova Hedwigia Beiheft 136: 55–69.
- RYNEARSON, T.A.; NEWTON, J.A. & ARMBRUST, E.V. (2006): Spring bloom development, genetic variation, and population succession in the planktonic diatom *Ditylum brightwellii.* Limnology and Oceanography 51: 1249–1261.
- Salzburger, W.; Ewing, G.B. & von Haeseler, A. (2011): The performance of phylogenetic algorithms in estimating haplotype genealogies with migration. Molecular Ecology 20: 1952–1963.
- SIVER, P.A. (1991): The Biology of *Mallomonas*: Morphology, Taxonomy and Ecology. 230 pp., Kluwer Academic Publishers, Dordrecht.
- SIVER, P.A. & WOLFE, A.P. (2005): Eocene scaled chrysophytes with pronounced modern affinities. – International Journal of Plant Sciences 166: 533–536.
- SIVER, P.A.; LOTT, A.M. & WOLFE, A.P. (2009): Taxonomic significance of asymmetrical helmet and lance bristles in the genus *Mallomonas* (Synurophyceae) and their discovery in Eocene lake sediments. – European Journal of Phycology 44: 447–460.
- SIVER, P.A. (2015a): Synurophyte algae. In: WEHR, J.D.; SHEATH, R.G & KOCIOLEK, J.P. (eds): Freshwater Algae of North America. 2nd ed. 607 pp., Academic Press, San Diego.
- SIVER, P.A.; Jo, B.Y.; KIM, J.I.; SHIN, W.; LOTT, A.M. & WOLFE, A.P. (2015b): Assessing the evolutionary history of the class Synurophyceae (Heterokonta) using molecular, morphometric, and paleobiological approaches. – American Journal of Botany 102: 921–941.
- SIVER, P.A.; SKOGSTAD, A. & NEMCOVA, Y. (2019): Endemism, palaeoendemism and migration: the case for the 'European endemic', *Mallomonas intermedia*. – European Journal of Phycology 54: 222–234.
- SIVER, P.A. (2023): Tracing lineages of scale–bearing Chrysophyceae over geologic time. Fottea 23: 164–176.
- ŠKALOUD, P.; KYNČLOVÁ, A.; BENADA, O.; KOFROŇOVÁ, O. & ŠKALOUDOVÁ, M. (2012): Toward a revision of the genus *Synura*, section Petersenianae (Synurophyceae, Heterokontophyta): morphological characterization of six pseudo—cryptic species. Phycologia 51: 303–329.
- ŠKALOUD, P.; KRISTIANSEN, J. & ŠKALOUDOVÁ, M. (2013):

 Developments in the taxonomy of silica–scaled chrysophytes from morphological and ultrastructural to molecular approaches. Nordic Journal of Botany 31: 385–402.
- ŠKALOUD, P.; ŠKALOUDOVÁ, M.; PROCHÁZKOVÁ, A. & NĚMCOVÁ, Y. (2014): Morphological delineation and distribution patterns of four newly described species within the *Synura petersenii* species complex (Chrysophyceae, Stramenopiles). European Journal of Phycology 49: 213–229.
- ŠKALOUD, P.; ŠKALOUDOVÁ, M.; DOSKOČILOVÁ, P.; KIM, J.I.; SHIN, W. & DVOŘÁK, P. (2019): Speciation in protists: Spatial and ecological divergence processes cause rapid species diversification in a freshwater chrysophyte. Molecular Ecology 28: 1084–1095.
- ŠKALOUD, P.; ŠKALOUDOVÁ, M.; JADRNÁ, I.; BESTOVÁ, H.; PUSZTAI, M.; KAPUSTIN, D. & SIVER, P.A. (2020): Comparing morphological and molecular estimates and pigment composition of *Synura* of species diversity in the freshwater genus *Synura* (Stramenopiles): A model for understanding diversity of eukaryotic microorganisms. Journal of Phycology 56: 574–591.

- ŠKALOUD, P.; JADRNÁ, I.; DVOŘÁK, P.; ŠKVOROVÁ, Z.; PUSZTAI, M.; ČERTNEROVÁ, D.; BESTOVÁ, H. & RENGEFORS, K. (2024): Rapid diversification of a free–living protist is driven by adaptation to climate and habitat. Current Biology 34: 1–14.
- STAMATAKIS, A. (2014): RAXML version 8: a tool for phylogenetic analysis and post–analysis of large phylogenies.

 Bioinformatics 30: 1312–1313.
- STELBRINK, B.; JOVANOVSKA, E.; LEVKOV, Z.; OGNJANOVA-RUMENOVA, N.; WILKE, T. & ALBRECHT, C. (2018): Diatoms do radiate: evidence for a freshwater species flock. Journal of Evolutionary Biology 31: 1969–1975.
- STOKES, A.C. (1885): Notices of new Fresh–Water Infusoria.—
 III. The American Monthly Microscopical Journal
 7: 121–127.
- STRÖMBERG, C.A. (2011): Evolution of Grasses and Grassland Ecosystems. – Annual Review of Earth and Planetary Sciences 39: 517–544.
- Tahvanainen, P.; Alpermann, T.J.; Figueroa, R.I.; John, U.; Hakanen, P.; Nagai, S. et al. (2012): Patterns of Post–Glacial Genetic Differentiation in Marginal Populations of a Marine Microalga. PLoS ONE 7: e53602.
- Wee, J.L.; Fasone, L.D.; Sattler, A.; Starks, W.W. & Hurley, D.L. (2001): ITS/5.8S DNA sequence variation in 15 isolates of *Synura petersenii* Korshikov (Synurophyceae).

 Nova Hedwigia Beiheft 122: 245–258.
- WERDELIN, L. & LEWIS, M.E. (2013): Temporal Change in Functional Richness and Evenness in the Eastern African Plio–Pleistocene Carnivoran Guild. PLoS ONE 8: e57944.
- White, T.; Bruns, T.; Lee, S. & Taylor, J. (1990): Amplification and direct sequencing of fungal ribosomal RNA Genes for phylogenetics. In book: PCR Protocols and Applications A Laboratory Manual. pp. 315–322, Academic Press.

Supplementary material

The following supplementary material is available for this article:

Table S1. Strains used in this study and the GenBank accession numbers for their nu SSU rDNA, nu LSU rDNA, pt LSU rDNA, pt psaA, pt rbcL, and nu ITS rDNA gene sequences. Newly generated accessions are given in bold.

This material is available as part of the online article (http://fottea.czechphycology.cz/contents)

© Czech Phycological Society (2025) Received May 18, 2025 Revised June 24, 2025 Accepted June 25, 2025 Published online September 3, 2025